Reports

Nitric Oxide Air Pollution: Detection by Optoacoustic Spectroscopy

Abstract. *Nitric oxide is detected by a new technique in which tunable infrared radiation from a spin-flip Raman laser is used to measure the absorption spectrum of a gas sample by optoacoustic spectroscopy. This technique is sensitive enough to detect a concentration of 0.01 part per million of nitric oxide pollution in air samples.*

The application of a new technique for air pollution detection has allowed us to measure nitric oxide concentrations as low as 0.01 ppm with a gas volume of $\lesssim 1$ cm^3 and a measurement time of ~ 4 seconds. In this technique the tunable radiation from a spin-flip Raman laser (*1*) is used to measure the infrared absorption spectrum of a gas sample by optoacoustic spectroscopy (*2*). The technique is general enough to be used for the detection of various other gaseous pollutants.

Nitrogen oxides are important pollutants (*3*) in automobile as well as power plant exhausts. The relevance of these oxides to smog production because of their absorption of ultraviolet radiation is well established. Traditionally, detection of gaseous air pollutants is carried out with wet chemical techniques. In particular, NO is detected (*4*) by its conversion to NO_2 and its final absorption in acid permanganate solution. The change in the color of the acid permanganate solution is detected with a spectrophotometer and is indicative of the NO concentration. There are three major drawbacks of the wet chemical methods: (i) Each pollutant requires a different set of techniques; (ii) a relatively large volume of the gas to be analyzed is required; and (iii) the amount of time required to achieve a reasonable sensitivity.

Thus a scheme is needed whereby a number of different pollutants can be analyzed rapidly and with reasonable sensitivity even in the presence of large concentrations of other gases. Measuring infrared absorption is a useful technique because almost all of the known pollutants have their fundamental absorption bands in the infrared portion of the spectrum from ~ 2 to 15 μm. The problem of interference from other gases is present, but each gas has its own absorption "fingerprint," and it is always possible to find at least one absorption line of the pollutant which is not overlapped by nearby absorption lines from other gases. Thus the source of infrared radiation used for measurement should have sufficient resolution to distinguish between pollutant absorption and interfering absorption. A second problem of detection of pollutants by infrared absorption is that for typical pollutant concentrations of 1 ppm at atmospheric pressures, the infrared absorption is too small to be measured by direct determination of transmission through a reasonable path length. Optoacoustic spectroscopy solves both of these problems and has allowed us to detect NO concentrations of less than 1 ppm.

The measurement of small optical absorptions (at low pollutant concentrations) is accomplished (*2*) by using the optoacoustic effect (the calorimetric method) in the pollutant. This method of detection involves the use of a cell containing the gaseous pollutant through which periodically interrupted infrared radiation passes. If the wavelength of the infrared radiation coincides with the wavelength of an absorption line, a periodic heating of the gas takes place. The resulting pressure fluctuations are detected by a capacitor microphone placed in the cell. Kreuzer (*2*) has described this technique and has shown that the sensitivity is limited by the Brownian motion of the microphone diaphragm, and that the method is capable of detecting absorbed powers as small as 10^{-9} watt.

The optoacoustic technique for very low gas concentrations requires infrared radiation of high intensity and monochromaticity (*2*). Thus a laser source is needed at the absorption wavelength of the pollutant. At random, it is very difficult to find a good coincidence of known laser lines (even though there are an enormously large number of them) with absorption lines of pollutants. In addition, to distinguish between the absorption line of the pollutant and the background absorption caused by some other gas, it is desirable to measure the absorption of the gas as a function of wavelength. In short we need a source of coherent infrared radiation. Of the various ways of generating tunable coherent radiation, we have chosen to use the spin-flip Raman laser (*1*) which gives us tunable radiation in the 5- to 6-μm range and in the 9- to 14-μm range. The spin-flip Raman laser consists of a pump laser, at a fixed optical frequency ω_0, which

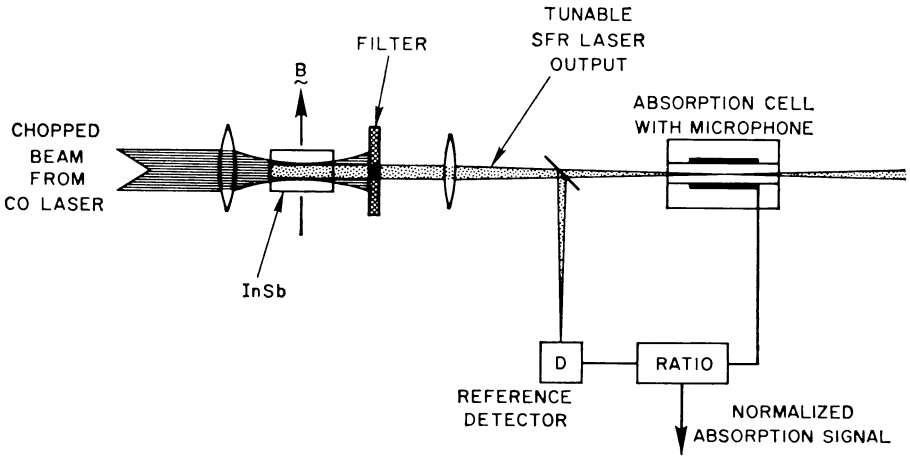

Fig. 1. Experimental setup for air pollution detection by optoacoustic absorption measurement using a spin-flip Raman laser.

is focused into a sample of InSb in a variable magnetic field, B, to generate the tunable Raman laser radiation at frequency ω_s given by

$$\omega_s = \omega_o - g\mu_B B \qquad (1)$$

where g is the g value of electrons in InSb, and μ_B is the Bohr magneton (*1*). This source has been used for conventional high-resolution spectroscopy (*5*) and thus should be ideal for pollution detection in conjunction with the microphone absorption detector.

Figure 1 illustrates the experimental setup. The amplitude-modulated pump radiation is obtained from a liquid N_2–cooled carbon monoxide laser operating continuously on the P (12) transition of the $8 \rightarrow 7$ vibration band of CO at 1888.31 cm^{-1}. The average pump power is about 0.7 watt. This radiation is focused with a lens into a 2 by 2 by 4 mm InSb sample in a magnetic field as shown. The tunable spin-flip Raman laser radiation, resonated collinearly with the pump laser beam, emerges from the InSb sample along with the unused pump radiation. A dielectric-coated filter rejects the pump radiation and allows the tunable spin-flip Raman radiation to pass. An average spin-flip Raman laser power output of ~ 50 mw was obtained and could be tuned from 1843 to 1788 cm^{-1} by changing the magnetic field from ~ 20 to ~ 55 kgauss. The spin-flip Raman laser power is focused with a lens into the microphone absorption cell containing the gas to be analyzed. About 15 mw of the tunable laser power enters into the cell. A beam splitter gives a reference on the output power level (measured with a photoconductive detector) and is used to normalize the signal output from the absorption cell. This normalized signal is then plotted as a function of the magnetic field which tunes the output frequency of the spin-flip Raman laser. The magnetic field values are converted into frequency values according to the tuning relation given in Eq. 1.

In order to demonstrate the usefulness of the technique in detecting air pollution, we have chosen to measure nitric oxide in a number of gas samples by analyzing them in the range from 1810 to 1825 cm^{-1} (by varying the magnetic field from ~ 30 to ~ 40 kgauss). Figure 2A shows the absorption spectrum of 20 ppm of NO in N_2 at a total pressure of ~ 300 torr obtained with an integration time of 1 second. (All the traces in Fig. 2, except for Fig. 2B, were obtained with an integration time of 1 second.) The lines numbered 1, 5, 6, 8, and 11 are identified as NO absorption lines by their frequencies (*6*) as well as by their relative intensities (Table 1). The remaining lines arise from water vapor absorption (*7*). Figure 2B shows the signal output from the cell when the spin-flip Raman radiation was blocked from entering the cell (the sensitivity scale is expanded by a factor of 100 and the integration time is now 4 seconds). The cell noise output is about 1/2000 of the NO absorption signal in Fig. 2A for 20 ppm of NO in N_2. This indicates that NO concentrations as small as 0.01 ppm can be detected. The widths of the lines in Fig. 2A are limited by pressure broadening; at the pressure used in the present measurements (300 torr), this broadening can be estimated to be of the order of 0.1 to 0.2 cm^{-1}.

Table 1. Identification of NO absorption lines in Fig. 2.

Line number	Frequency	Identification
1	1824.33 cm^{-1}	Π 1/2, P(15 1/2)
5	1820.44	Π 1/2, P(16 1/2)
6	1818.74	Π 3/2, P(16 1/2)
8	1816.56	Π 1/2, P(17 1/2)
11	1814.69	Π 3/2, P(17 1/2)

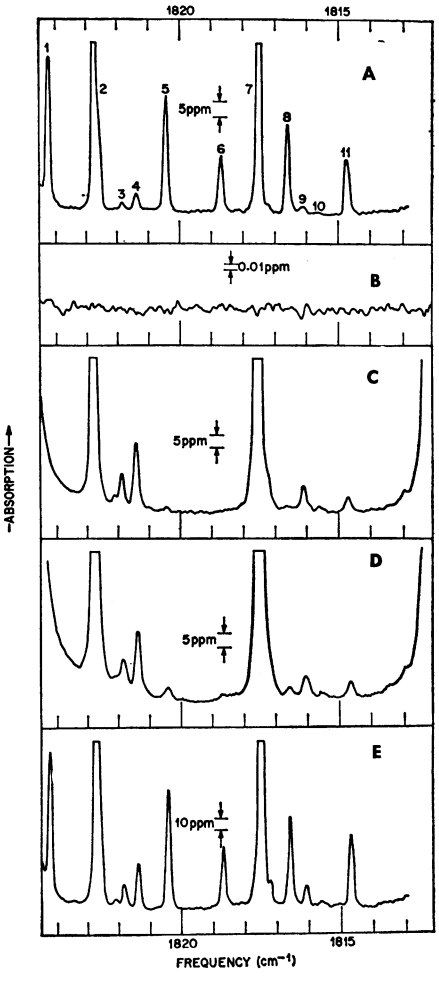

Fig. 2. Absorption spectra of various gas samples in the range of 1815 to 1825 cm^{-1} obtained by changing the magnetic field from 30 to 40 kgauss. All spectra are taken at a pressure of 300 torr. (A) Calibration spectrum of 20 ppm NO in N_2. Lines numbered 1, 5, 6, 8, and 11 are due to NO (see Table 1). The remaining lines are due to H_2O. Vertical sensitivity is 1.0; integration time is 1 second. (B) Absorption cell noise. Vertical sensitivity is 100; integration time is 4 seconds. (C) Room air at 21°C and 30 percent relative humidity. Vertical sensitivity is 1; integration time is 1 second. (D) Air sample from Route 22 near Plainfield, N.J. Vertical sensitivity is 1.0; integration time is 1 second. (E) Automobile exhaust. Vertical sensitivity is 0.4; integration time is 1 second.

Figure 2C shows the absorption spectrum of room air (21°C, 30 percent relative humidity) also taken at 300 torr. Water vapor absorption is very strong in the 1815 to 1825 cm^{-1} region, and because of the interference from these strong water vapor lines, not all of the NO lines seen in Fig. 2A can be conveniently used for monitoring NO concentration. Thus we pick the lines 6 and 8 for monitoring NO pollution. We see that the laboratory room air exhibits a NO concentration of ~ 0.1 ppm, so that measurements of ambient NO levels are possible with an integration time of 1 second. Figure 2D shows the analysis of a sample of air collected near a busy road at about 8:00 p.m. during moderately heavy traffic. The increase in NO concentration due to the automobile traffic is clearly visible. The NO concentration is measured to be ~ 2 ppm.

Figure 2E shows the absorption spectrum of a sample of automobile exhaust from a decelerating Bell Telephone Laboratories fleet car. The sensitivity is now decreased by a factor of 2.5 compared to that in Fig 2, A, C, and D. The amount of NO in the exhaust is in excess of 50 ppm, and this measurement shows the wide dynamic range of our technique. However, even at these high concentrations, there is no saturation of the output signal from the microphone cell as the NO concentration increases. The upper limit of linearity is set by the considerations

of maintaining a uniform power level of the tunable radiation through the microphone cell in the presence of the absorption by the gas. Thus, even up to NO concentrations high enough to give an absorption of $\sim 10^{-2}$ through the microphone cell, the signal output from the microphone cell will be linear with respect to NO concentration. The saturation and nonlinear behavior of the output signal is not expected to take place until we reach NO concentrations in excess of 10^4 ppm.

Our technique of determining NO pollution in air samples requires only ~ 1 cc of gas sample for an analysis that is capable of detecting 0.01 ppm of NO with a 4-second integration time, and thus this method can be adapted to real time measurement of NO pollution even at ambient levels. With longer integration times, the lower limit for NO detection can be improved. For detection of source pollution, significantly shorter integration times can be used. Many different pollutants can be detected with this technique and the method has a large dynamic range. We have already detected NO_2 in some experiments and we expect to investigate other pollutants with our technique.

L. B. KREUZER
Bell Telephone Laboratories, Inc.
Murray Hill, New Jersey 97974
C. K. N. PATEL
Bell Telephone Laboratories, Inc.
Holmdel, New Jersey 07733

References

1. C. K. N. Patel and E. D. Shaw, *Phys. Rev. Lett.* **24**, 451 (1970); *Phys. Rev.* **B3**, 1279 (1971); E. D. Shaw and C. K. N. Patel, *Appl. Phys. Lett.* **18**, 215 (1971); C. K. N. Patel, *ibid.*, p. 274; A. Mooradian, S. R. J. Brueck, F. A. Blum, *ibid.* **17**, 481 (1970); S. R. J. Brueck and A. Mooradian, *ibid.* **18**, 229 (1971).
2. L. B. Kreuzer, *J. Appl. Phys.*, in press.
3. A. C. Stern, Ed., *Air Pollution* (Academic Press, New York, ed. 2, 1968), vol. 3, chaps. 32 and 33.
4. ———, *ibid.*, vol. 2, chap. 17.
5. C. K. N. Patel, E. D. Shaw, R. J. Kerl, *Phys. Rev. Lett.* **25**, 8 (1970).
6. T. C. James and R. J. Thibault, *J. Chem. Phys.* **41**, 2806 (1964).
7. W. S. Benedict and R. F. Calfee, "Line parameters for 1.9 and 6.3 micron water vapor bands," *ESSA Professional Paper 2* (U.S. Department of Commerce, Washington, D.C., 1967).

12 May 1971

Alpha-Recoil Thorium-234: Dissolution into Water and the Uranium-234/Uranium-238 Disequilibrium in Nature

Abstract. *The rate of ejection of alpha-recoil thorium-234 into solution from the surface of zircon sand gives an alpha-recoil range of 550 angstroms. The alpha-recoil thorium-234 atoms ejected into the groundwater may supply excess uranium-234. In pelagic sediments, ejected alpha-recoil thorium-234 may contribute to the supply of mobile uranium-234 in the sedimentary column.*

A radioactive disequilibrium state between ^{238}U and ^{234}U has been observed by many workers both in seawater and in freshwater (*1*). Many samples of freshwater show enrichments of ^{234}U rather than deficiencies. The mechanism of the fractionation of ^{234}U with respect to its radiogenic parent ^{238}U in natural waters has been discussed in connection with the physiochemical nature of α-recoil atoms in the silicate lattice (*2*).

The α-recoil atoms in the silicate lattice are thought to be more easily leached out than the atoms that have settled into the lattice positions at the time of crystallization of the silicate. Thus it is plausible that the addition of excess ^{234}U atoms to freshwater is attributable to the leaching of α-recoil ^{234}U atoms in the weathering process of natural silicate. However, in laboratory leaching experiments on fresh igneous rocks or minerals, solutions containing ^{234}U have been found to contain less than 1.3 times the equilibrium amount of ^{238}U (*3*). Therefore, the process responsible for a disequilibrium state between ^{234}U and ^{238}U in nature with an activity ratio of ^{234}U to ^{238}U as high as 3 or 4 would require mechanisms other than the selective dissolution of α-recoil ^{234}U atoms. The process of dissolution of ^{234}Th atoms produced by the α-decay of ^{238}U atoms located near the surface of the solid silicate particles may be one of the other mechanisms responsible for the disequilibrium.

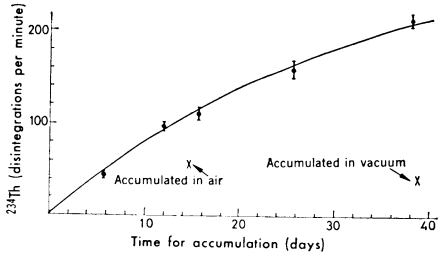

Fig. 1. Amount of ^{234}Th accumulated in the aqueous phase by the ejection of α-recoil ^{234}Th from the surface of the zircon powder suspended in the solution.

The observed increase in the amount of ^{234}Th in the aqueous phase of a system consisting of fine zircon powder and diluted nitric acid or sodium carbonate solution is shown in Fig. 1. The suspension containing 50 g of zircon powder (particles about 1 to 10 μm in diameter) was allowed to stand for a predetermined period of time. The amounts of nuclides leached out were measured in the solution after separation from the mineral powder and in the washing solution, 0.3*N* nitric acid. The uranium and thorium contents of zircon sand are 360 parts per million (ppm) and 131 ppm, respectively. The surface area of the 50 g of powder was estimated from microscopic observation of the particles to be 1.8×10^5 cm^2.

In this experiment, the size of the particles (1 to 10 μm) is large enough as compared with the range of the α-recoil atoms, and we can neglect the curvature of the surface of the particle. Thus the rate of supply Q of ^{234}Th atoms from the solid surface to the solution is given by

$$Q = \frac{1}{4} LSu\rho\lambda_8 \qquad (1)$$

where L is the α-recoil range of ^{234}Th in the silicate, S and ρ are, respectively, the surface area and the density of the silicate, u is the number of ^{238}U atoms in 1 g of silicate, and λ_8 is the decay constant of ^{238}U. The accumulated amount A of ^{234}Th in the solution after time t is given by

$$A = \frac{1}{4} LSu\rho\lambda_8(1 - e^{-\lambda_4 t})/\lambda_4 \qquad (2)$$

where λ_4 is the decay constant of ^{234}Th. The observed increase in the amount of ^{234}Th in the aqueous phase, which is shown in Fig. 1 (*4*), fits the calculated increase predicted by Eq. 2 on the basis of an α-recoil range of 550 Å. This range is in good agreement with the estimated range which has been discussed in connection with investigations of the fossil α-recoil tracks in silicate (*5*). The accuracy of this observed range depends primarily on the accuracy of the estimation of the surface area of the mineral powder and may have an error of about 10 percent.